

SpaceOps-2025, ID # 475

May 2024 Space Weather Events and their Impact on Spacecraft Operations

Myrto Tzamali^a, Judit Palacios^b, Alexi Glover^{a,e*}, Federico Da Dalt^b, Hannah Laurens^b, Andrew Monham^c, Richard Broughton^c, Hugh Evans^d, Ralf Keil^b, Juha-Pekka Luntama^a

^a *Space Weather Office, Space Safety Programme, European Space Operations Centre (ESA/ESOC), Darmstadt, Germany*

^b *Starion for ESA, Europaplatz 4, 64293 Darmstadt, Germany*

^c *EUMETSAT, Eumetsat Allee 1, 64295 Darmstadt, Germany*

^d *European Space Research & Technology Centre, ESA/ESTEC, Keplerlaan 1 NL-2200 AG Noordwijk*

^e *ESA Headquarters, 8-10 Rue Mario Nikis, CS 45741, 75738 Paris Cedex 15, France*

* Corresponding Author

Abstract

During the first half of May 2024, a period of intense space weather activity resulted in the largest recorded geomagnetic storm in 20 years and widespread auroral observations reported in both hemispheres. This period included multiple major flares, several Earth-directed coronal mass ejections (CMEs), and solar energetic particle events, all of which affected spacecraft operations through different mechanisms. In October 2024 another severe geomagnetic storm (G4 classification) also affected satellite operations. These two space weather events were detected by both space agencies and commercial satellite operators during routine operations, with satellites in low Earth orbit experiencing increased atmospheric drag. In response to these events, some commercial operators reported that they temporarily paused Earth observation imaging, and satellite communication services were also impacted, as reported by operators in media statements. This paper will describe the key space weather events observed during this period and their implications for spacecraft operations as we enter the peak of Solar Cycle 25, drawing from the experience of ESA and EUMETSAT mission operations. Since these events were the largest seen so far in the ongoing Solar Cycle 25, we briefly compare with the geomagnetic storms of October 2003, during the Solar Cycle 23, to assess the effectiveness of existing space weather monitoring and forecasting capabilities, considering the information available to spacecraft operators at the time and how it influenced their response strategies.

Keywords: space weather, atmospheric drag, radiation, geomagnetic storm

Acronyms/Abbreviations

AOCS: Attitude and Orbit Control Subsystems
CCD: Charged Coupled Device
CME: Coronal Mass Ejection
D3S: Distributed Space Weather Sensor System
ESA: European Space Agency
FD: Forbush Decrease
GCR: Galactic Cosmic Rays
GEO: Geostationary Earth Orbit
GLE: Ground Level Enhancement
ICME: Interplanetary Coronal Mass Ejection
IMF: Interplanetary Magnetic Field
LEO: Low Earth Orbit
LT: Local Time
MLAT: Magnetic Latitude
NGRM: Next Generation Radiation Monitor
PPE: Prompt-Particle Event Counter
SA: Solar Array
SAA: South Atlantic Anomaly
SEP: Solar Energetic Particle event
SEU: Single Event Upset
SWE: Space Weather Service Portal
UT: Universal Time

1. Introduction

Geomagnetic storms are large disturbances in the Earth's magnetosphere caused by interactions with solar wind and coronal mass ejections (CMEs) generated by the Sun. They impact the upper atmosphere, ionosphere, and magnetosphere across all latitudes and local times and can have a significant influence on space-borne and ground-based technological systems, notably satellites, by increasing air drag, surface charging, and radiation damage. While their effects vary by region-low, mid, or high latitudes-they are interconnected. The strength and nature of these effects depend on several factors: the ring current strength (seen in magnetic deflections), how far the auroral zone expands, how close the magnetopause moves to Earth, and how quickly the storm begins.

Two major geomagnetic storms occurred in May and October of 2024, marking significant periods of enhanced space weather activity. This paper presents key observations from the two

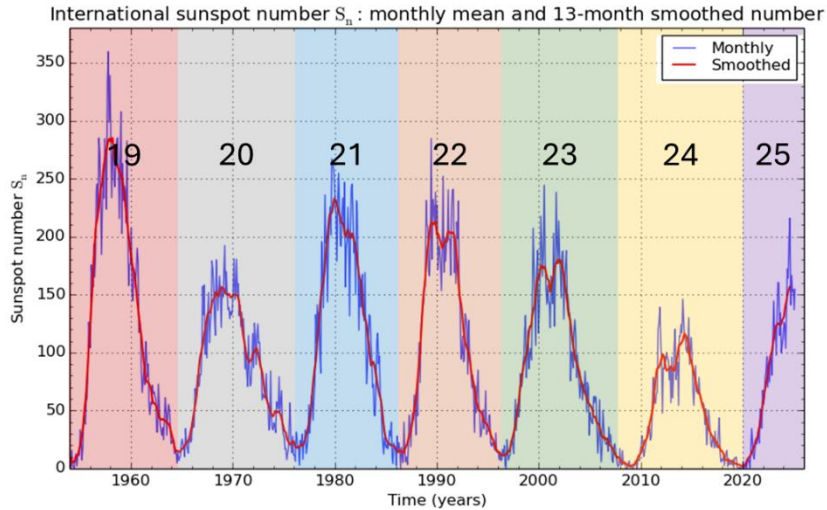
periods, drawing on data products available via ESA's Space Weather Service Network¹ along with feedback from ESA and EUMETSAT flight control teams on their experience during these periods. Reflecting on the fact that not all periods of enhanced activity may be considered extreme in all relevant environments, this study also places the 2024 events in the context of the October 2003 storm, which serves as a reference point due to its well-documented impact on spacecraft operations.

On May 11, 2024, we witnessed one of the most intense geomagnetic storms since 2003, often referred to as the "Gannon Storm" or "Mother's Day Storm". During this period, at least seven CMEs were observed, traveling at very high speeds, which resulted in a prolonged geomagnetic storm marked by a Sym-H index that reached -518 nT at 0214 UT and a $Dst=-412$ nT at 0200 UT making it the largest geomagnetic storm observed since 2003. This storm led to auroras being visible at unusually low latitudes and stayed significantly active with $Kp > 8$ for more than 24 hours. The space weather auroral events on May 10–11 have been reported as the third and sixth most extensive events on record from January 1650 – July 2024, respectively, with auroras observed at unusually low latitudes in both hemispheres. The most extensive auroral event remains the Chapman-Silverman Event on February 4, 1872 [1]. While recent analysis indicates that the storm's intensity corresponded to an expected statistical return period of 1-in-12.5-year event, its duration aligned with a return period of 1-in-41-year event, highlighting its unusually long-lasting nature relative to its magnitude [2]. Due to its intensity, the event was widely detected by broadband seismic sensors worldwide. Magnetic signals associated with the storm were clearly evident in seismic data for over 55 hours, making it one of the longest geomagnetic storms ever recorded by such instruments [3].

The severe geomagnetic storm which occurred on October 10, 2024 at around 1520 UT, was caused by a fast CME associated with an X1.8-class solar flare, travelling at an average speed of 1200 km/s. Both storms excited the aurora visibility with the equatorward auroral boundary reaching 20° MLAT during the May storm [4,5] and 30° MLAT during the October event [6].

As Solar Cycle 25 approaches its maximum (Fig. 1), having begun in December 2019 and exhibiting a stronger cycle than initially predicted [7,8], this research examines the characteristics and operational impacts of two periods of enhanced space weather activity. It investigates their solar origins, the resulting magnetospheric responses, and their implications for satellite operations while also assessing the extent to which space weather events can disrupt satellite operations, highlighting the need for preparedness against potential operational risks.

¹ <https://swe.ssa.esa.int>



SILSO graphics (<http://sidc.be/silso>) Royal Observatory of Belgium 2025 March 1

Figure 1. The monthly mean sunspot number (blue) and the 13-month smoothed monthly sunspot number (red) for the last five solar cycles, illustrating the cyclic variation in solar activity. Data sourced from the **Royal Observatory of Belgium, SILSO** (<http://sidc.be/silso>), accessed on 1 March 2025. The coloured bands indicate the Solar Cycles from 1954 to 2026. The plot was retrieved from the ESA SWE Network Service Portal (<https://swe.ssa.esa.int/web/guest/sidc-S108-federated>).

2. May and October 2024 Storms

In this section, the characteristics of the two major geomagnetic storms of May and October 2024 will be discussed, along with reported impacts on satellite operations.

2.1 May 10-11 2024 Geomagnetic Event

In May 2024, a series of powerful solar flares and coronal mass ejections (CMEs) propelled clouds of charged particles and magnetic fields toward Earth, triggering the most intense geomagnetic storm in 20 years-and potentially one of the most remarkable auroral displays [9]. From May 5 to 15, 2024 19 major CMEs were observed from the Large Angle Spectroscopic Coronagraph onboard the ESA/NASA SOHO mission (SOHO/LASCO). The activity commenced on May 5, 2024, when active region No. 13664 (NOAA AR 3664) on the Sun generated an C7.5-class flare accompanied by multiple M-class flares, including the most intense X-class flare of the ongoing Solar Cycle 25 up to that point, a X8.7-class flare on May 14. This region was the largest sunspot group observed in over a decade [10]. The unique growth rate of this particular active region AR3664, along with its magnetic energy and strong non-neutralised electric currents, has been studied in Kontogiannis [11] and Jarolim et al. [12]. This region also ejected several coronal mass ejections (CMEs) from May 8th, which reached Earth on May 10, 2024, triggering an extreme geomagnetic storm according to the NOAA scale for geomagnetic storm categorisation. From 1800 UT on May 10 to 1800 UT on May 11, the Kp index remained over 8 for a full day and the SYM-H index indicated a sudden storm commencement around 1700 UT, followed by a main

phase that lasted for more than eight hours. On May 11, the Kp index peaked at a value of 9 between 0000 UT and 0300 UT and 0900 UT and 1200 UT. At 0214 UT on May 11, SYM-H dropped as low as -518 nT, and then began a gradual recovery extending into May 12. During the event the interplanetary magnetic field (IMF) recorded a peak strength of 73 nT, with its southward-oriented component along Earth's magnetic axis reaching -50 nT. Additionally, the solar wind exhibited moderately high density and speeds, ranging from 750 to 800 between May 10 and 11 (Fig.2). The Disturbance Storm Time index (Dst) plunging to -412 nT on May 11, as reported by Kyoto's World Data Center for Geomagnetism [13], made it the strongest geomagnetic storm since the Halloween storm of 2003, which recorded a minimum Dst index of -422 nT [14-16] and the sixth greatest starting from 1957 when continuous measurement of the Dst index began [13]. The daily international sunspot number increased dramatically from 119 on May 1 reaching 206 on May 6 (Fig.1).

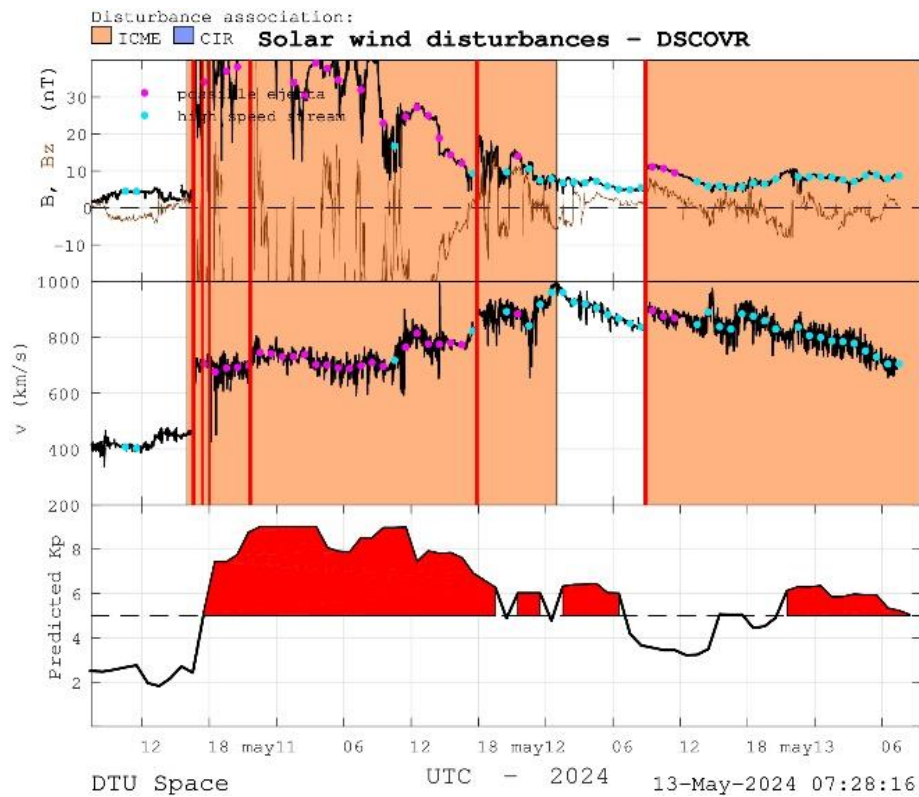


Figure 2. May 10-12, 2024: **Top panel:** Plot from DTU AWARE (<https://swe.ssa.esa.int/dtu-aware-federated>) showing the interplanetary magnetic field (IMF) observed by the near real-time operational spacecraft DSCOVR at L1. The total intensity B_t is shown in black, and the B_z component in brown. **Middle panel:** Solar wind speed measured at L1. The red vertical lines indicate significant interplanetary shocks. Orange shading highlights disturbances caused by interplanetary CMEs. The light blue and pink dots mark disturbed intervals used to trace the solar origin of each disturbance. Pink dots indicate possible CME ejecta, while light blue dots denote high-speed stream material. **Bottom panel:** Kp forecast from DTU AWARE (<https://swe.ssa.esa.int/dtu-aware-federated>). The Kp forecast is based on the past three hours of solar wind observations. Red markers highlight intervals when the predicted Kp reaches storm levels.

2.1.1 Forecasting of the Event

Regarding the Kp forecast for the event, three products are featured as part of ESA’s Space Weather Service Network. The first displayed is DTU AWARE, which provides a Kp forecast shown in the bottom panel of Fig. 2 above. The second is a product from IRF, which uses the IRF-Kp-2017 model and includes a comparison with real-time Kp values from GFZ (left panel in Fig. 3). The third is a forecast developed by BGS which provides predictions of the Kp index for the next 72 hours, using autoregressive linear models based on the K_{GBI} time series (bottom right panel in Fig.3). As such, Kp reached twice the maximum value of 9 on May 11, as shown in the plot of the definitive Kp data in Fig. 3. Regarding the Dst index, the SolarHoldover product from the University of Alcalá (bottom left panel in Fig.3) displays the Dst data (green curve) alongside the modelled recovery phase of the storm (blue curve). The product shows that the model effectively captured the recovery phase, accurately estimating the magnetosphere’s recovery time from the storm’s minimum. However, the fit is slightly less accurate due to the storm’s multi-step structure.

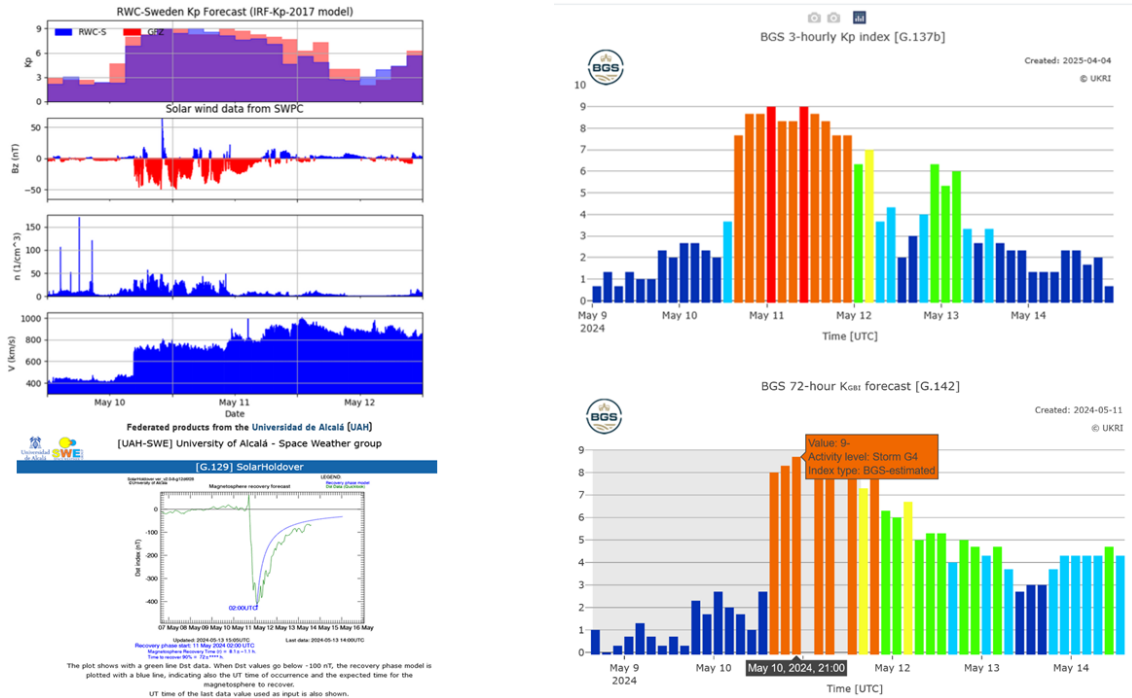


Figure 3. Top Left panel: Forecast of the 3-hour Kp index based on the IRF-Kp-2017 model (<https://swe.ssa.esa.int/irf-federated>). The model is driven by real-time solar wind data from NOAA SWPC. The top sub-panel displays the forecasted Kp values (blue bars) alongside the real-time Kp values from GFZ (red bars). The three sub-panels below show the measured 1-minute solar wind magnetic field Bz (positive values in blue, negative values in red), particle density n, and speed v. **Bottom Left panel:** The SolarHoldover product from UAH displays the Dst index (green) along with the modelled recovery phase (blue). The model estimated the recovery time of the magnetosphere (<https://swe.ssa.esa.int/web/guest/uah-senmes-federated>). **Top right panel:** The 3-hour Kp index provided by BGS (<https://swe.ssa.esa.int/web/guest/BGS-federated>). **Bottom Right panel:** Forecast of the 3-hourly K_{GBI} index for the next 72 hours (<https://swe.ssa.esa.int/web/guest/BGS-federated>). The plot includes both forecast and estimated data, with a grey background indicating the section that is not part of the forecast.

The UKMO Near-Earth Space Weather Notifications product² and the SIDC Daily Space Weather Bulletin³ successfully forecasted the severe geomagnetic storm and accurately predicted the arrival of multiple interplanetary coronal mass ejections (ICMEs) from active region AR13664 that would impact Earth on May 10. The first CME was detected at 1639 UT, causing an abrupt increase in solar wind speeds to approximately 700 km/s. A second, stronger CME followed at 2139 UT, further increasing solar wind speeds to a peak of 804 km/s, as reported by the UKMO Notifications. The arrival of these 2 CMEs is in agreement with observations [17,18].

In addition to regular bulletins and event-based notifications, the ESA SWE Service Network also includes a number of tailored products characterising and forecasting the Earth’s trapped radiation environment designed to help satellite operators assess the possible impacts of space weather events on their systems. The following plot shows the SaRIF⁴ product group capturing the impact of the geomagnetic storm on the population of relativistic electrons in the Earth’s radiation belts including a significant injection of electrons into the slot region on May 10 which then decays over the following days.

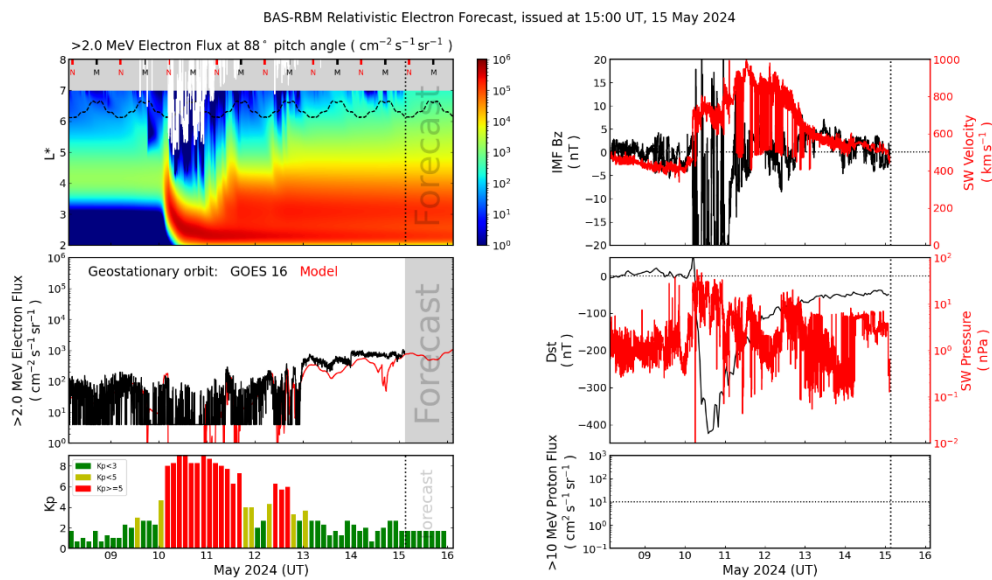


Figure 4. May 8th – 16th 2024: **Top Left Panel:** The electron flux as a function of L^* —the distance from the centre of the Earth along the equatorial plane, measured in Earth radii—and time. The GOES-16 satellite’s location is marked for reference by a black dashed line. Magnetic noon and midnight local times (MLT) are indicated along the top of the plot. Periods when the outer boundary of the geomagnetic field lies within $L^* = 8$ are highlighted by a solid white line. **Middle Left Panel:** The $>2.0\text{MeV}$ electron flux at the location of the satellite, comparing measurement data and model output. **Bottom Left Panel:** The K_p index colour coded based on the activity level. **Top Right Panel:** Solar wind velocity measured by DSCOVR (red) and the B_z component of the IMF (black). **Middle Right Panel:** Solar dynamic pressure measured by DSCOVR (black) and the Dst index (black). **Bottom Right Panel:** Proton flux greater than 10MeV measured by GOES spacecraft (no data available for the selected period).

² <https://swe.ssa.esa.int/metoffice-alerts-e-federated>
³ <https://swe.ssa.esa.int/web/guest/sidc-S110-federated>
⁴ <https://swe.ssa.esa.int/sarif-federated>

The RB-IND product group⁵ federated by ONERA, currently presented via the ESA SWE Service Network on a demonstration basis, provides access to several effects indices targeting satellite operators. These provided the following initial assessment for the May events, with surface and internal charging risks indicated to remain elevated for a period of 7-8 days following onset on May 11.

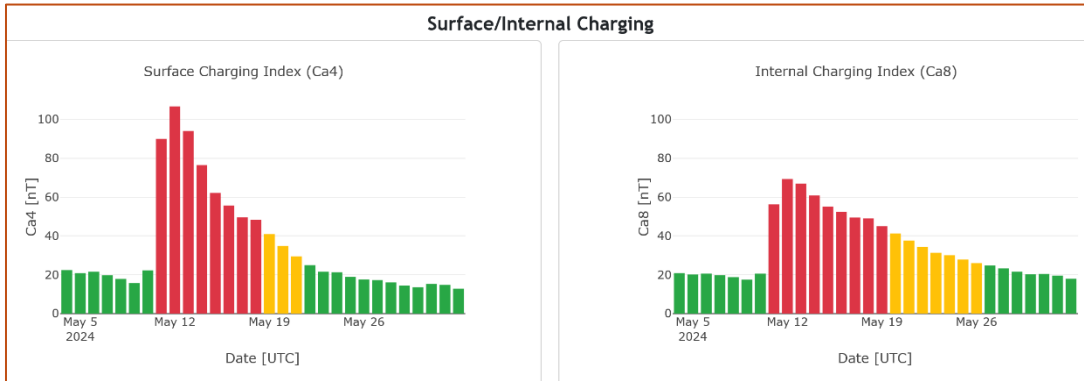


Figure 5. ONERA RB-IND assessment of the potential for radiation induced impacts on satellite operations during the May 2024 events.

2.1.2 Radiation Environment and Impact on Satellites

On May 11, a Ground-Level Enhancement (GLE) was detected following an X5.8-class solar flare. In response, the GLE++ alert product⁶ generated a warning and multiple watch alerts based on data from neutron monitor stations. Figure 6, shows the readings from several neutron monitors, clearly indicating a significant increase in the flux of high-energy solar particles reaching Earth's atmosphere. The left panel of Fig. 6 presents the status of neutron monitor stations across the network. The summary panel on the left indicates that 4 stations exceeded the Alert level early on May 11, suggesting a moderate but noticeable GLE event.

The Multi-station neutron monitor data from_Neutron Monitor Database Network (NMDB) initially recorded the ICME's arrival at Earth (right panel of Fig. 6), triggering a Forbush Decrease (FD)—a phenomenon in which background Galactic Cosmic Rays (GCR) levels temporarily diminish due to the ICME interaction. This decrease coincided with the onset and initial phases of the geomagnetic storm, as described by Mavromichalaki et al. [19]. Additionally, the data captured GLE #74 associated with the X5.8 flare occurring a few hours later, around 0200 UT on May 11, visible in the neutron monitor data plot as a distinct, smaller peak that slightly overlaps and comes after the Forbush decrease.

⁵ <https://swe.ssa.esa.int/onera-rb-ind-federated>

⁶ <https://swe.ssa.esa.int/web/guest/anemos-federated>

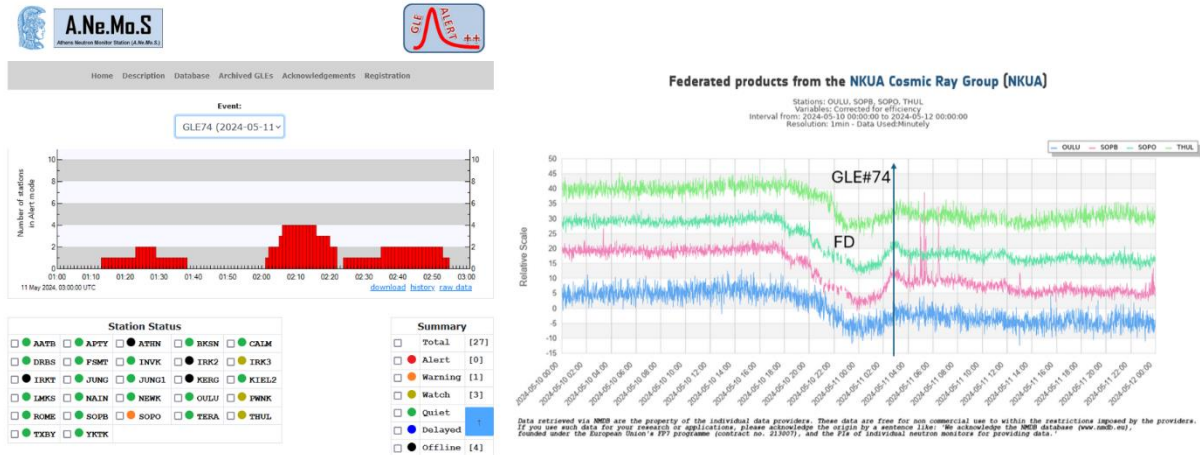


Figure 6. Left panel: Detection of Ground-Level Enhancement (GLE74) on May 11, 2024, following the X5.8 solar flare, as recorded by the ANeMoS. GLE++ alert product. The GLE++ alert product issued a GLE email alert at 0205 UTC based on the ANeMoS server timestamp (<https://swe.ssa.esa.int/web/guest/anemos-federated>). **Right panel:** 1-min data from multiple stations detecting increased cosmic ray activity.

The ESA Space Safety Programme’s Next Generation Radiation Monitor (NGRM) hosted payload onboard Sentinel-6 provided continuous monitoring of the trapped radiation environment during the May space weather events. The radiation data measured by Sentinel-6 in LEO show a significant increase across all channels (5 MeV, 9 MeV, 50 MeV, and 73 MeV) during both the May and October events, with the increase being more pronounced in the lower-energy channels (Fig. 7). The comparison between L ~1.4 and L ~2 during the May event shows that the average proton fluxes (normalized to the first 30 days of January 2024, for comparison purposes) experienced the highest increase at L ~1.4, particularly in the 50 MeV (medium energy protons) and the 73MeV (high energy protons). On the other side, the average proton fluxes at L ~2 show an increase on the lowest energy levels and a decrease on higher energy levels during the May event. The increase during October event is visible too. The discrepancy between the low and higher energies is due to the trapping in the magnetic field. Higher energy particles require a stronger field, which is found at lower altitudes, while the lower energy particles can be trapped in the weaker field at higher altitudes. Also, the lower energy channels suffer from high energy proton contamination, so the signal of lower energy particles at lower altitudes (L ~1.4) that correlate with the higher energy channel contains a significant contribution from high energy protons. For accurate interpretation of the data, it should be noted that the detector is not fully aligned with the pitch angle distribution (90°) but rather captures only a portion of it.

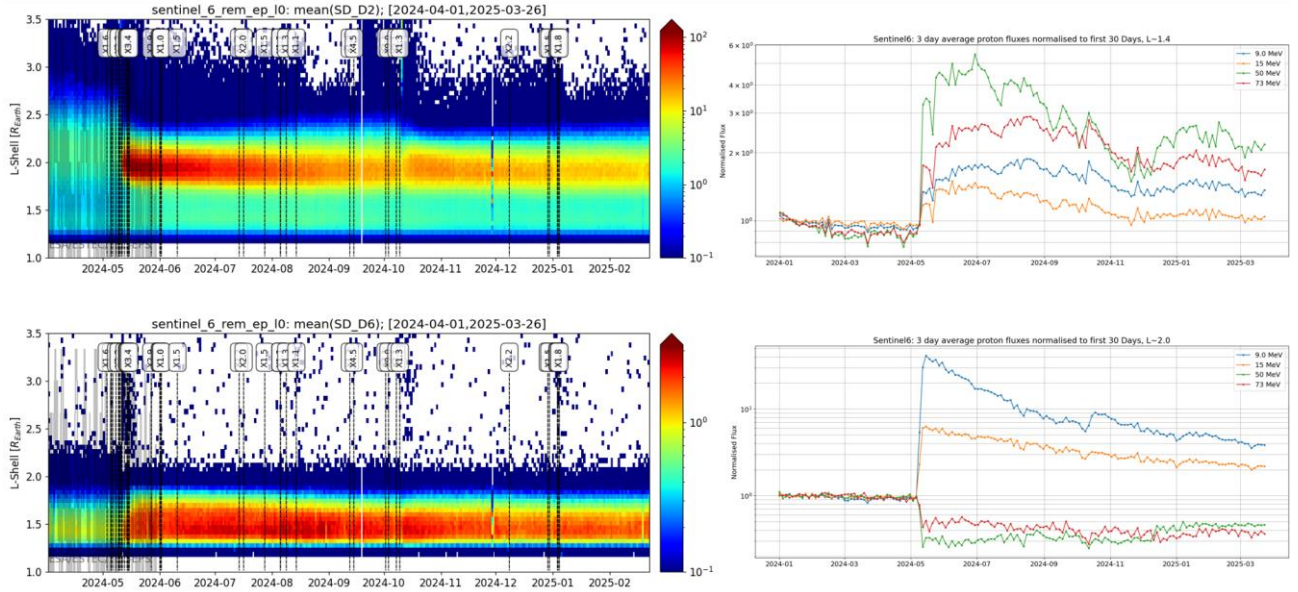


Figure 7. Radiation data from NGRM onboard Sentinel-6 from May 2024- February 2025. **Left panel:** Spectrograms of the energy fluxes at 9MeV channel (top) and at 73MeV (bottom). **Right panel:** 3-day average proton fluxes normalized to the first 30 days of January 2024 at L=1.4 (top) and L=2.0 (bottom).

The ESA Space Safety Programme’s Next Generation Radiation Monitor onboard EDRS-C in GEO monitored the proton differential fluxes as seen in Fig. 8 (left panel). The proton flux as measured in GEO by GOES is shown in Fig. 8 (right panel) and they show that the May event passed the S2 level for a small period of time. Interestingly, also GOES observed an extreme magnetospheric compression that briefly pushed the bow shock below GEO orbit. During this event, GOES-18 detected the shocked interplanetary magnetic field (IMF) outside the magnetopause, within the magnetosheath region [18].

The SREM unit onboard the PROBA-1 mission provides high-resolution measurements of the charged particle radiation environment, with direct discrimination between electrons, protons, and heavy ions. The instrument did not collect any data, with data collection resuming 14 days later. In Fig.9, radiation measurements from the SREM unit onboard the Integral mission are shown from May 8th to May 17th for channels 8, 12, and 15. The 4 high peaks in the data are due to the satellite's highly elliptical orbit, which passes through perigee approximately every three days. Channel 12 (blue line) is sensitive to both protons and electrons, while Channel 15 is sensitive to protons only. Channel 8 (orange line) is known as a coincident channel, which is insensitive to electrons; a dominant signal appears when the satellite enters the proton belt. When Channels 12 and 15 align (as on May 14), it indicates that the signal is dominated by protons. In contrast, when they diverge, it suggests the presence of an electron signal contaminating the measurements. It can be seen from the graph that the May storm had a strong impact, leading to an increase in radiation levels. The measurements returned to their nominal state after almost a week. Integral's orbit only encountered the outer edges of the proton belt at this time, with a minimum L of ~ 2.6 . This is within the low energy trapped proton belt, but not deep enough to encounter the newly formed trapped proton belt.

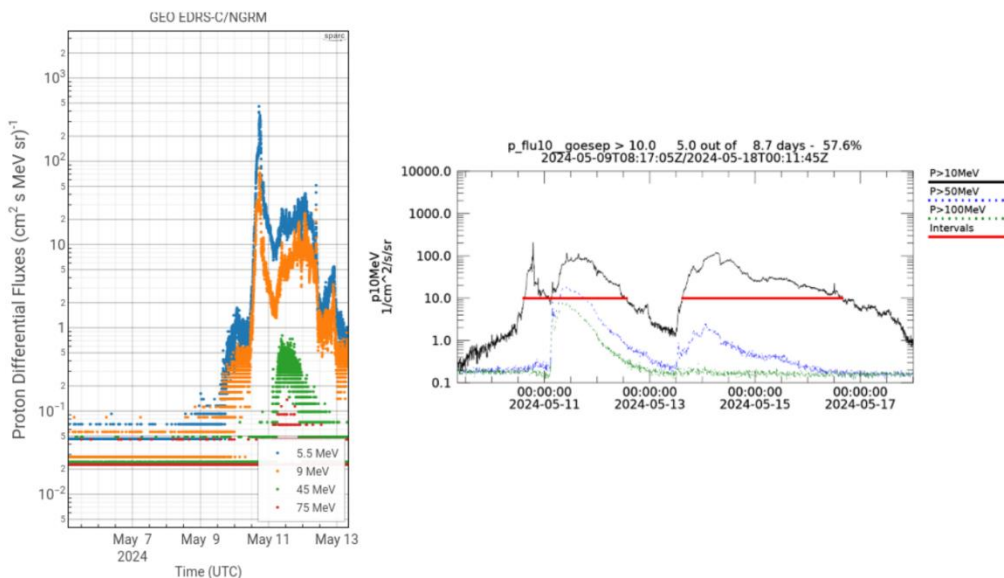


Figure 8. Left panel: ESA NGRM data (measured at GEO orbit) proton differential fluxes during the May storm from product SPARC EDRS-C NGRM L2 proton differential fluxes (<https://swe.ssa.esa.int/sparc-geo-ngrm-r171-federated>) from May 6 to May 13, 2024. Right panel: Proton flux measured by GOES shown from H-ESC statistical products (<https://swe.ssa.esa.int/ral-hparc-stat-federated>) from May 10-17, 2024, where the S1 level is marked with a red line.

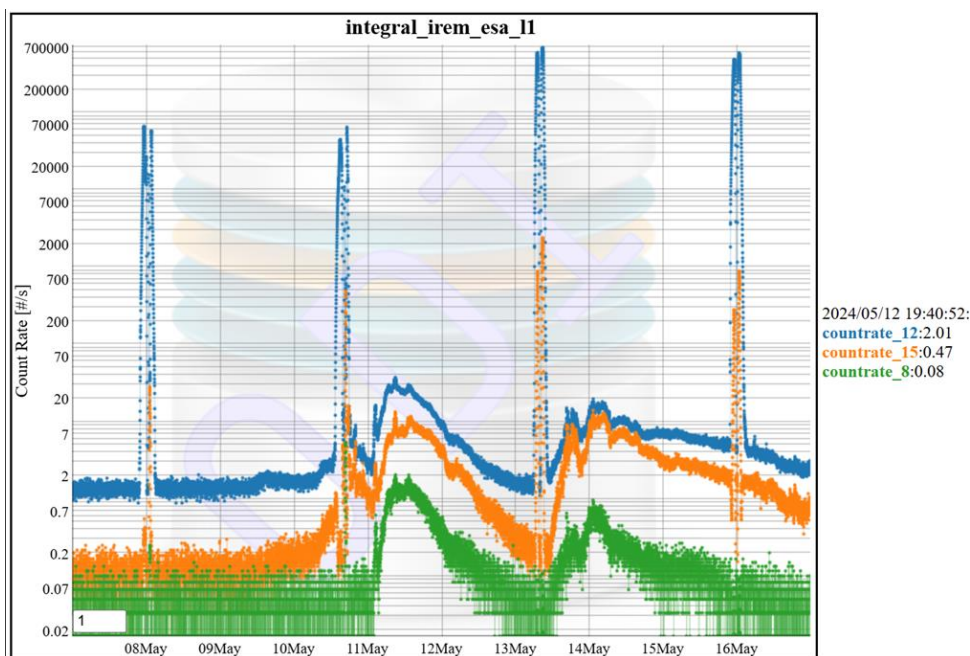


Figure 9. Radiation measurements from the Integral mission. Three different channels are shown: Channel 12 (blue), Channel 15 (orange), and Channel 8 (green). The satellite passes its perigee every three days, leading to the high spikes in the measurements observed on May 10th, 13th, and 16th.

Despite the fact that the May event was the most significant period of enhanced space weather activity of the Solar Cycle 24 so far, ESA mission flight control teams consulted in the preparation of this paper reported very little disruptions to their operations. There were no major consequences reported in onboard electronics, navigation systems, or satellite communications. Atmospheric drag led to some missions in LEO experiencing a deviation from the control deadband resulting from increased atmospheric drag, resulting in the need for significantly bigger than normal orbit control movements due to a higher number of collision warnings which is a recurring difficulty during the current solar maximum [20]. The main takeaway from this event is that, of those ESA missions consulted, current spacecraft designs and operational procedures for solar maximum have demonstrated good resilience.

The Gaia spacecraft's 'billion-pixel camera' relies on a series of 106 charge coupled devices (CCDs) – sensors that convert light into electrical signals. In May, the electronics controlling one of these CCDs failed – Gaia's first CCD issue in more than 10 years in space [21]. While the root cause for the failure is not entirely clear, it has been linked to the May 2024 space weather event occurring at the same time (Fig.10). While CCD electronics are known to be radiation-sensitive, these devices had been operating flawlessly for over 10 years. The Gaia operations team observed the failure occurring a few days after the storm, with no prior signs of degradation or malfunction. The failure was sudden, without any detectable decay or warning indicators. Regrettably, the affected CCD was deemed unrecoverable.

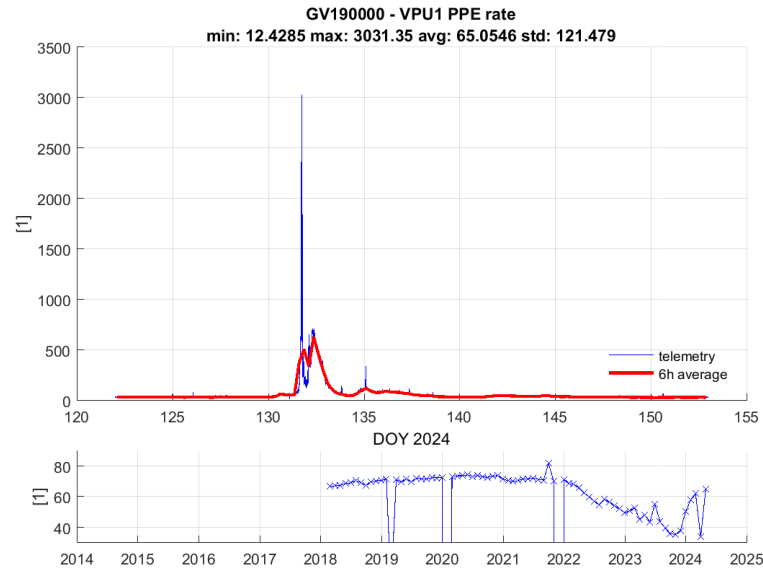


Figure 10. Gaia mission, PPE monitor: VPU1 PPE rate during the May 2024 geomagnetic storm. The top panel shows prompt-particle event data (blue) and the 6-hour average of the PPE prompt-particle-event (red), highlighting a significant spike around Day of Year (DOY) 131–133 (May 10–12, 2024), corresponding to the peak of the event. The bottom panel provides historical context, showing variations in PPE rates over the past decade. The extreme increase in particle precipitation rates aligns with the radiation storm detected during the event.

EUMETSAT reported that the Space Environment Monitor (SEM-2) instruments on-board the MetOp satellites experienced an alert status on May 11, marking one of only four red status events recorded since 2012. Previous occurrences include 7 Jan 2014 (X1.2 flare and SEP event), 10 Sep 2017 (X8.2 flare, SEP event and GLE#72), and 28 Oct 2021 (X1 flare and SEP event, which led to an SEU in the IASI OBDH memory). A minor spacecraft attitude instability was observed. The AOCS system responded by activating reaction wheels, followed by magnetorquers to offload excess momentum. The primary impact on MetOp systems was increased atmospheric drag due to elevated solar flux, resulting in a faster-than-normal orbital decay as thermospheric density increased. As shown in Fig. 11, the protons detected by the SEM-2 instrument on the MetOp satellites during the geomagnetic events of March 7, 2012 and May 11, 2024 indicate that the proton fluxes originating from solar flares are significantly lower than those observed during South Atlantic Anomaly (SAA) crossings. Also reported in the literature, the METOP/MEPED observed increased fluxes inside the proton radiation belts after 11 May [10].



Figure 11. 70MeV proton flux measurements from the SEM-2 instrument onboard MetOp satellites during the geomagnetic storm on May 11, 2024. The plot distinguishes between increased proton fluxes associated with polar solar storm activity and those detected during South Atlantic Anomaly (SAA) transits. The SAA-related fluxes exhibit significantly higher intensities compared to those originating from solar events.

Despite the very good satellite resilience demonstrated by the ESA and EUMETSAT flight control teams, within the wider spacecraft operations community, certain events were reported in the literature that warrant mention and a number of publications highlight experiences of operators during this period, highlighting that despite the resilience described above, continuous space weather monitoring and improved nowcasting and forecasting remain crucial for satellite operations.

For example, the May 2024 storm was reported to have resulted in increased air drag on satellite orbits with for example KANOPUS-V3 (SATCAT 43180) experienced an orbital decay up to four times greater than normal, reaching as much as 180 km per day [22,23].

2.2 5-13th October 2024 Geomagnetic Event

The solar activity was high during this period in general. The solar radio flux index F10.7 - index used as a proxy of the EUV forcing and input for thermospheric models - on October 3 was amongst the highest values of the Solar Cycle 25 so far, around 312 sfu, from CLS⁷.

The main CMEs of the period relevant for the event were Earth-directed CMEs, on October 3 and October 9, which originated from active areas AR3842 and AR3848. The first CME, associated with an X9 flare at the Sun on October 3, arrived at the Earth on October 6 and triggered the main phase of a major geomagnetic storm from 2200 UT on October 6 to 0800 UT on October 8, reaching Kp of 7, as shown on the plot of Kp in Fig. 12 (right bottom panel). Before the storm could fully recover, another CME triggered a severe geomagnetic storm on October 10. This CME, ejected on 9 October 2024 at 0212 UT, associated with a X1.8 flare and with an estimated speed of 1900 km/s as reported by the product SIDC Daily Space Weather Bulletin⁸, impacted Earth on 10 October at around 1500 UT. A sudden increase in solar wind pressure resulted in a storm sudden commencement (SSC) of 41 nT at 1600 UT on October 10, followed by a gradual decrease in the *Dst* index, reaching a minimum of -341 nT at 0200 UT on October 11. The maximum Kp index during the storm reached 8+. The main phase lasted approximately 10 hours—shorter, yet comparable to the duration of the May 2024 storm. Despite these similarities, the May event was stronger, as indicated by higher Kp and *Dst* indices. This difference in intensity is further supported by the fact that the May storm was driven by multiple CMEs, whereas the October storm was associated with just one. Figure 12 shows that the IMF *Bz* component remained reasonably stable near zero between 0000 and 1200 UT on October 10, gradually increasing to around 10 nT after a brief period of negative values earlier that day. Around 1515 UT, a CME shock was evident in ACE and DSCOVR, causing a storm to begin suddenly. Shortly after the shock, *Bz* reached -20 nT. The solar wind speed reached almost 800 km/s, similarly to the May event. GOES magnetometer data showed that three substorms followed, characterized by wide local time extent and quasiperiodic oscillations are known as sawtooth events [24-26].

⁷ <https://swe.ssa.esa.int/web/guest/cls-federated>

⁸ <https://swe.ssa.esa.int/web/guest/sidc-S110-federated>

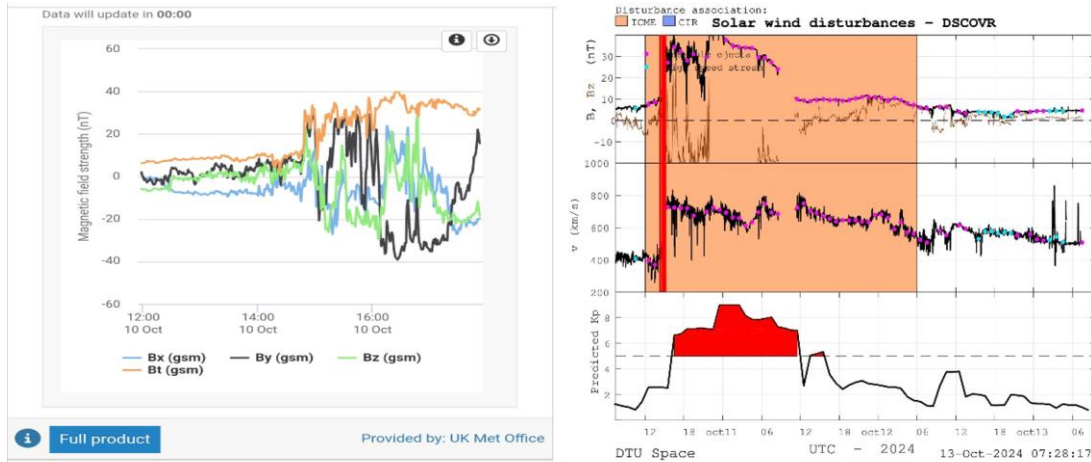


Figure 12. October 10-13, 2024: **Left panel:** The product UKMO Near-Earth NRT solar wind SW/L1 product (<https://swe.ssa.esa.int/metoffice-sw-l1-federated>) shows the arrival of the CME displaying the high and variable magnetic field components in the ICME. **Right Top panel:** Plot from DTU AWARE (<https://swe.ssa.esa.int/dtu-aware-federated>) showing the interplanetary magnetic field (IMF) observed by the near real-time operational spacecraft DSCOVR at L1. The total intensity B_t is shown in black, and the B_z component in brown. **Right Middle panel:** Solar wind speed measured at L1. The red vertical lines indicate significant interplanetary shocks. Orange shading highlights disturbances caused by interplanetary CMEs. The light blue and pink dots mark disturbed intervals used to trace the solar origin of each disturbance. Pink dots indicate possible CME ejecta, while light blue dots denote high-speed stream material. **Right Bottom panel:** K_p forecast from DTU AWARE (<https://swe.ssa.esa.int/dtu-aware-federated>). The K_p forecast is based on the past three hours of solar wind observations. Red markers highlight intervals when the predicted K_p reaches storm levels.

2.2.1 Forecasting of the event

The October geomagnetic storm associated with the full-halo CME at 0230 UT on October 9, was accurately predicted for its arrival on 10 October. SIDC Daily Space Weather Bulletins⁹ reported several CMEs: on October 7, a CME was ejected and forecasted only to produce a glancing blow at Earth. CMEs ejected on October 8 did not reach Earth as forecasted. On 9 October, the very fast CME associated with an X1.8 flare, was forecasted to arrive on midday of 10 October.

The K_p index, provided by GFZ, on October 11 reached 8+, in agreement with the forecasted K_p index provided by DTU AWARE (bottom-right panel of Fig. 12) and the forecast from IRF (top left panel of Fig. 13). The recovery phase of the storm began at 0100 UT, as accurately forecasted by UAH, and is shown in the bottom right panel of Fig. 13. Compared to the May event, the recovery time was forecasted more accurately for the October event, due to its lower complexity.

⁹ <https://swe.ssa.esa.int/web/guest/sidc-S110-federated>

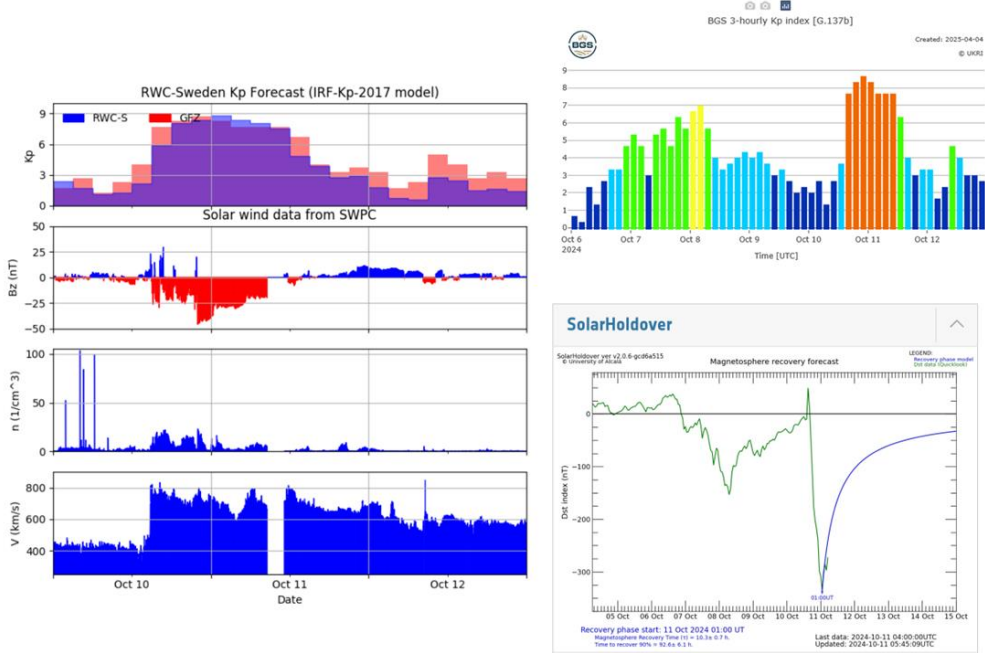


Figure 13. Left panel: Forecast of the 3-hour Kp index based on the IRF-Kp-2017 model (<https://swe.ssa.esa.int/irf-federated>). The model is driven by real-time solar wind data from SWPC. The top sub-panel displays the forecasted Kp values (blue bars) alongside the real-time Kp values from GFZ (red bars). The three sub-panels below show the measured 1-minute solar wind magnetic field Bz (positive values in blue, negative values in red), particle density n, and speed v. Top right panel: The 3-hour Kp index provided by BGS (<https://swe.ssa.esa.int/web/guest/BGS-federated>). Bottom Right panel: The SolarHoldover product from UAH, which displays the Dst index (green) along with the modelled recovery phase (blue). The model successfully estimated the recovery time of the magnetosphere (<https://swe.ssa.esa.int/web/guest/uah-senmes-federated>).

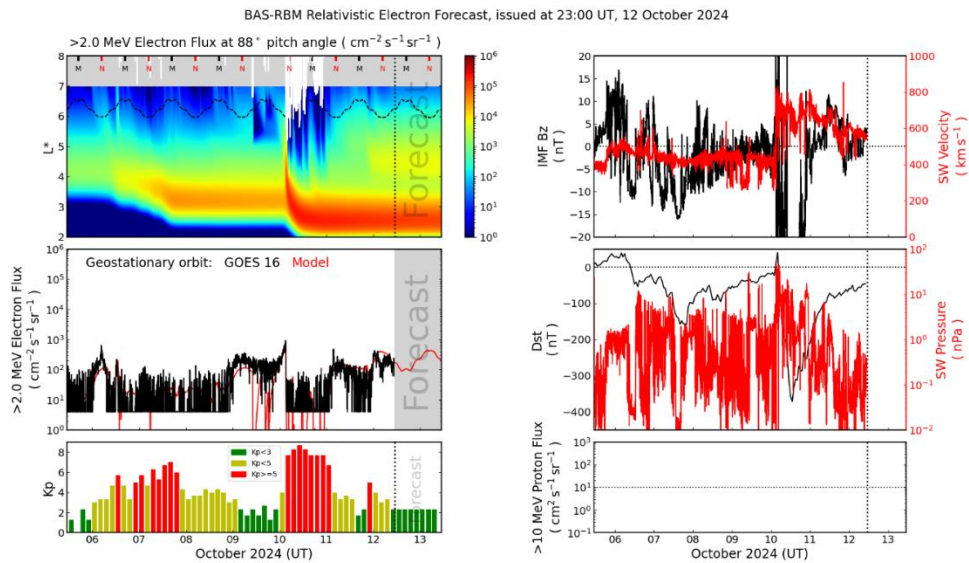


Figure 14. October 6- 13, 2024: SaRIF modelled impact of the October geomagnetic storm on the relativistic electron environment in Earth's orbit (<https://swe.ssa.esa.int/sarif-federated>). Left panel: The model along with modelled and observed environment in GEO (comparison with GOES 16 data), Kp. Right panel: The solar wind and IMF observations and the Dst index.

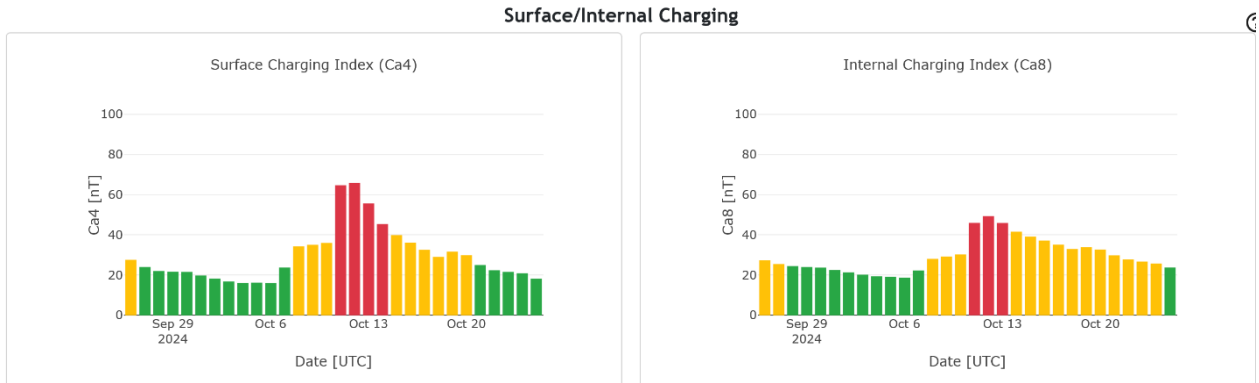


Figure 15. ONERA RB-IND estimated risk indices for the October 2024 events (<https://swe.ssa.esa.int/onera-rb-ind-federated>).

Figure 14 provided from the SaRIF product group indicates the effect of the October geomagnetic storm on the relativistic electron environment in Earth orbit. The top left panel in Fig. 14 presents model results and forecast evolution. Figure 15 above illustrates ONERA RB-IND product group predicted an increased risk of surface and internal charging due the October geomagnetic storm, but less pronounced than that estimated for the May 2024 event.

2.2.2 Radiation environment and impact on satellites

The GOES proton flux measurements from July 2024 to February 2025 show many SEP events, with the most activity occurring in October 2024. Figure 16 (left) is extracted from H-ESC statistical products¹⁰. The first energetic particle flux increase within this time frame was associated with an X2.1 solar flare on October 7th. However, this increase did not meet the NOAA S1 radiation storm threshold. A stronger occurrence occurred on October 9, when an X1.8 flare at around 0200 UT triggered a radiation proton storm that peaked at S1-S2 levels before briefly reaching S3 some hours later, continuing until October 10, as shown in Fig.16 (left panel). The red lines represent the S1 radiation storm proton flux threshold. When comparing the October and May 2024 SEP cases, the radiation storm in October had greater proton flux levels, with one flare associated with SEP peak >10MeV proton flux exceeding the S3 event threshold. By comparison, SEP events taking place in May 2024 reached S2 levels for >10MeV protons but may have been energetic enough to relate to a GLE, as discussed above. Neutron monitor records are not shown for the October 2024 event, since no GLE was registered.

The PPE monitor data from the Gaia mission reveals a sharp increase in particle detection rates, as shown in Fig. 16 (right panel). Notable increases are observed between October 6 and 16 (DOY 280–290), with a pronounced peak around DOY 284 (October 10), corresponding to the SEP event that began on October 9. Another period of elevated particle detection occurs between October 26 and 31 (DOY 300–305), aligned with the SEP event that started on October 24.

¹⁰ <https://swe.ssa.esa.int/ral-hparc-stat-federated>

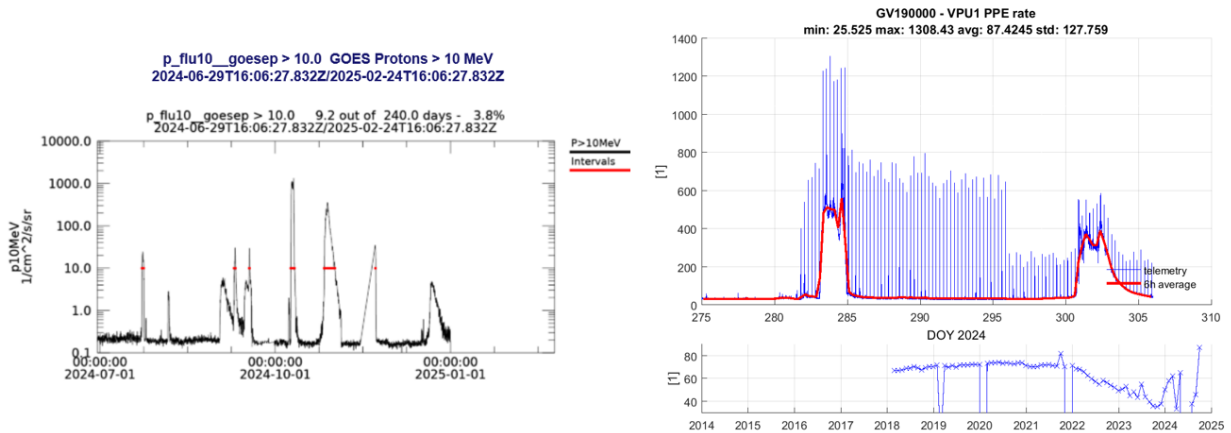


Figure 16. *Left panel:* GOES proton flux (> 10 MeV) from July 2024 to February 2025, displaying several solar energetic particle event (SEP) occurrences (<https://swe.ssa.esa.int/ral-hparc-stat-federated>). The red markers show times when proton flux exceeded the S1 radiation storm threshold. Notably, the October 2024 storm had the most severe activity, with proton flux exceeding the S3 (>1000) radiation storm. **Right panel:** Gaia PPE (prompt-particle event) monitor displaying VPU1 PPE rate over time. The top panel shows PPE data (blue) with a 6-hour average (red), highlighting periods of increased activity. Significant peaks are observed around DOY 280–290 (6–16 October) and additionally DOY 300–305 (26–31 October) in 2024. The bottom panel provides a long-term trend, showing variations in PPE rate from 2018 to the end of 2024.

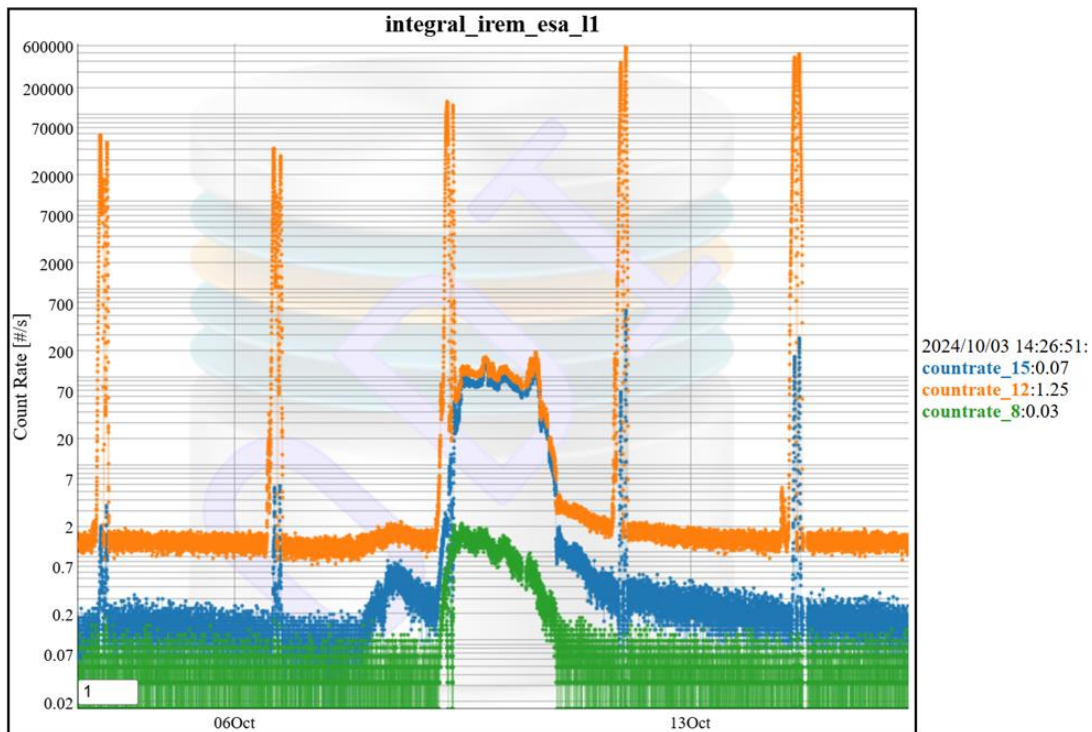


Figure 17. Radiation measurements from the Integral mission. Three different channels are shown: Channel 12 (blue), Channel 15 (orange), and Channel 8 (green). The satellite passes through perigee approximately every three days, resulting in the five prominent spikes observed in the measurements.

Measurements of proton fluxes from the ESA Next Generation Radiation Monitor onboard Sentinel-6 in LEO indicated an increase in flux in the lower energy levels as discussed in the previous section in Fig. 7. Similarly to the May event, Proba-1 did not collect any count rate

measurements during the October storm, from October 10 to October 18th. Radiation measurements from the Integral mission (Fig. 17) show a higher count rate compared to the May event. During the October storm, the count rate remained consistently around 70 for two days, in contrast to the May event (Fig. 8), where it peaked around 35 and lasted for less than a day.

Although the October storm lasted only 11 hours—shorter than the May event, which exceeded 24 hours—the unusually long development phase of the October storm has still been associated with noticeable disturbances to satellite operations [27,28]. It has been reported that a sharp altitude decay was observed in the Starlink-1089 satellite, which re-entered Earth’s atmosphere on October 12—approximately ten days earlier than expected. This accelerated re-entry could be linked to increased atmospheric drag, although further analysis may be needed to confirm the underlying cause [28].

According to EUMETSAT, the satellites exhibited robust resilience throughout the October event, with no notable impacts recorded. Similarly, ESA mission operators reported high resilience, and no major issues were reported by the flight control teams consulted in preparation of this paper.

Concerning the thermospheric densities, published on the Swarm dissemination server¹¹, during the storm events, the densities derived from accelerometer measurements [29] onboard the GRACE-FO mission [30], which measures the gravity field of the Earth in a near polar orbit at an altitude of approximately 480 km, showed peaks at 0500 local time (LT) and 1700 LT. The peak in thermospheric densities during the May event persisted longer than during the October event. In both cases, the cooling effect of the atmosphere was evident, as shown by a subsequent decrease in density following the initial peak. Interestingly, as shown in Fig. 18, thermospheric densities prior to the May storm were half the amplitude of those observed before the October storm, which can be attributed to the typical increase in densities during the equinoxes. The May event exhibits a more prolonged peak, while the October event shows a sharper but shorter-lived increase in density. The latitudinal distribution of densities for both events indicate values exceeding 4 kg/m³ across all latitudes. The higher increase in thermospheric densities observed during the May event is consistent with a greater energy input into the upper atmosphere, primarily driven by enhanced Joule heating [31, 38]. Estimates of Joule heating rates indicate that energy input during the October storm was lower than in May, supporting the conclusion that the May event was more intense [32]. Similar findings can be observed in the thermospheric densities derived from the accelerometer onboard the Swarm-C satellite, which orbits the Earth in a near polar orbit, at an altitude approximately 30 km lower than GRACE-C [38].

¹¹ <https://swarm-diss.eo.esa.int/#swarm%2FLevel2daily%2FLatest%2Fbaselines>

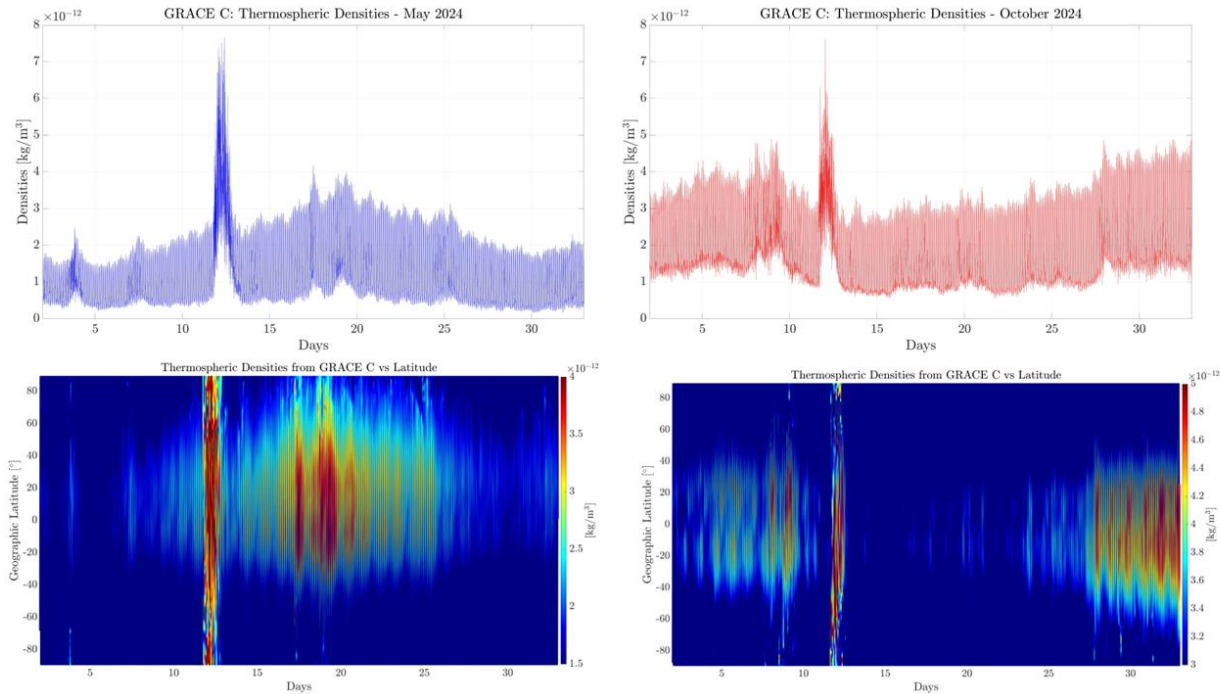


Figure 18. Thermospheric Densities Observed by GRACE-C During May and October 2024 Storm Events: **Top panels:** The time series of thermospheric densities derived from GRACE-C accelerometer measurements for May 2024 (left, blue) and October 2024 (right, red), with clear density peaks corresponding to geomagnetic storm activity. **Bottom panels:** The latitudinal distribution of thermospheric densities over time, highlighting the variation in density response across different geographic latitudes.

3. Comparison of the May and October Events with the Halloween Storm of 2003

The October 2003 solar storm, known as the Halloween Storm [33, 34], was extreme in many respects—not only because the geomagnetic storm reached the maximum level of G5 (Kp = 9), but also due to the intensity of solar activity, which included flares exceeding X17 [35], several extreme SEP events [15] and three GLEs. Between October 19 and November 7, 2003, a total of 80 coronal mass ejections (CMEs) and 143 X-ray flares were observed [36]. Among these, 17 X-ray flares were classified as significant events, and six distinct radiation proton storms were recorded, the strongest of which reached an S4 (severe) level on the NOAA space weather scale [37].

Two major geomagnetic storms occurred on October 29 and 30, 2003, as indicated by the Kp index (panel (a) in Fig. 19). GOES proton flux data show an increase of four orders of magnitude, marking S4 level, at 1200 UT on October 28, followed by an additional one-order-of-magnitude increase at 2100 UT on October 29 [36]. These were associated with 3 GLE on 28, 29 October and 2 November, now numbered events GLE#65, #66 and #67, as shown from the GLE+ product and the neutron monitor from NKUA (panels (c) and (d) in Fig. 19), as provided at ANEMOS

Federated¹². The maximum number of stations in alert mode from the GLE+ alert product was 12 on October 28, 6 on October 29, and 10 on November 2, 2003 (Figure 19, panel c)). The Service Assessment report for the Intense Space Weather Storms in 2003 [39] published by NOAA SEC (now NOAA/SWPC) summarises some of the main reported impacts of this period of extreme space weather conditions. The report indicates that the GSFC Space Science Mission Operations team reported that 59% of the Earth and Space Science spacecraft and 18% of the instrument groups experienced effects of the space weather activity. This included the loss of the MARIE instrument onboard the NASA Mars Odyssey mission. The report also notes that the ESA SMART-1 mission reported a total of 3 engine shutdowns due to radiation levels in lunar transfer orbit and Mars Express switched to using gyroscopes for stabilisation since the radiation storm resulted in the star trackers being unusable for a period of 15 hours. TV and Pay Radio satellite services were also impacted in a number of ways. Furthermore, EUMETSAT recorded a 1% drop in solar array current onboard one MSG satellite on October 28 which was attributed to solar activity. More recently, and as the on-orbit population increases, Berger et al. [40] revisited this period and the impact on satellite operations in LEO noting that “*For example, in the last extreme geomagnetic storm on record, the great Halloween Storm of 2003, anecdotal testimony from USAF operators during the storm recounts that the majority of LEO satellites were temporarily lost, requiring several days of around-the-clock work to reestablish the catalog.*”

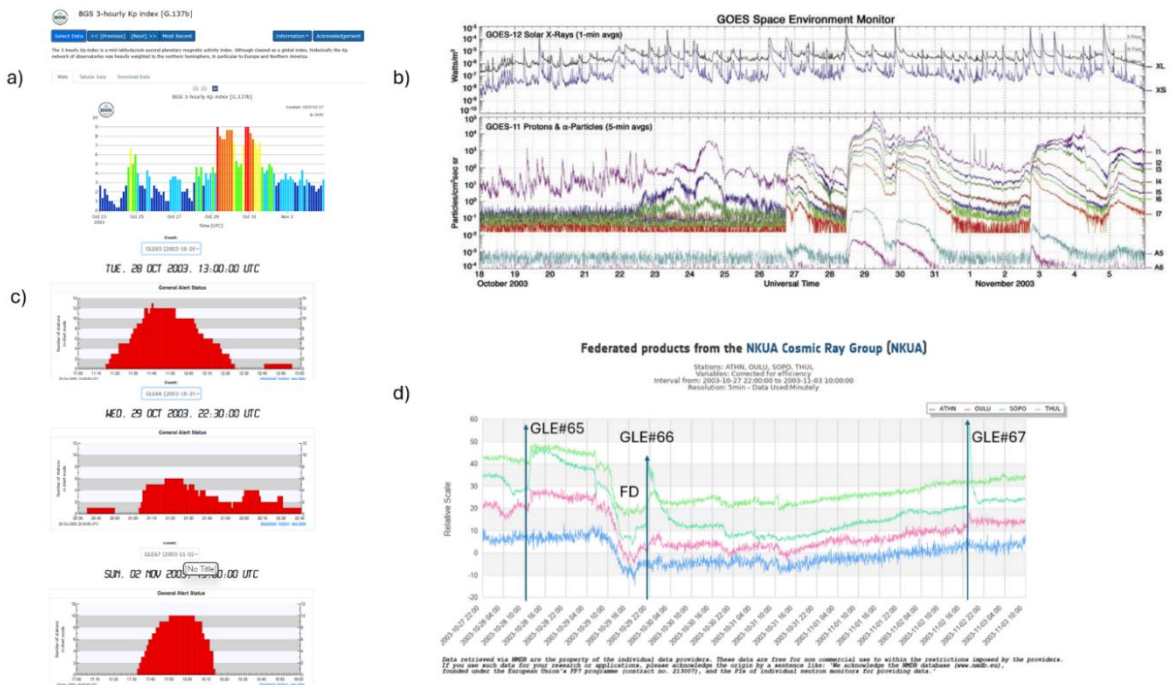


Figure 19. a): 3-hourly Kp index provided by BGS from October 23-November 3, 2003. b): GOES proton flux from October 18-November 5, 2003 [36]. c) number of alerts issued by the GLE+ alert product (<https://swe.ssa.esa.int/web/guest/anemos-federated>) in October 28, 29 and on November 2. d) 5 min data from multiple stations detecting increased Neutron Monitor measurements from October 27, 2003 to November 3, 2003 (<https://swe.ssa.esa.int/web/guest/anemos-federated>).

¹² <https://swe.ssa.esa.int/web/guest/anemos-federated>

Resilience to space weather conditions is an important factor in safe satellite design and operations and as certain orbits become increasingly populated accurate situational awareness is essential. The October 2003 "Halloween Storm" provides an important example of how major space weather events may produce radiation environments capable of impacting satellite integrity and mission continuity, with >10 MeV proton flux levels peaking at 29,500 pfu at geostationary orbit. Even more severe is thought to have been the Carrington Event of 1859, which may have reached proton fluxes as high as 200,000 pfu—levels far exceeding those experienced by today's satellite infrastructure.

4. Summary

The three major events presented in this study each triggered a different response in Earth's magnetic field and involved varying levels of complexity. The 2003 geomagnetic storm and the two major storms of 2024, which are examined in this paper, demonstrate that satellites in low Earth orbit (LEO) may be affected differently depending on their orbital characteristics and satellites in a range of orbits may show a wide range of responses to the radiation environment. Since each satellite in Earth's orbit observes the Earth at different local times, a geomagnetic storm can strongly impact one satellite while having little effect on another, even when they operate at similar altitudes. Understanding the distinct physical mechanisms behind each event is essential for assessing how satellites are affected and for improving storm impact forecasting and more research is needed to improve current models of the upper atmosphere and its response to space weather disturbances which can then be deployed in an operational context. Accurate models and tools are essential to help satellite operators prepare for such events—whether by adjusting orbital manoeuvres or entering alert mode. Therefore, analysing the different responses to each storm not only enhances our understanding of how space weather conditions impact the near-Earth environment, but also brings advances which will lead to improved space weather forecasts in future [41-43].

5. Conclusions

This paper presents an overview of the two major space weather events detected in 2024 and summarises impacts reported by spacecraft operators. ESA and EUMETSAT mission operators consulted in the preparation of this paper indicated a high level of resilience to the events and no negative impacts were reported.

In order to evaluate the events operational effects on satellites and draw attention to information available to support mission operations in predicting and responding to such disturbed conditions, this study examined the May and October 2024 events, two of Solar Cycle 25's most powerful geomagnetic storms so far, as well as the historic Halloween storms of 2003.

The results demonstrate that while the events observed in 2024 were detected in the increasingly populated Low Earth Orbit, the period of extreme space weather conditions observed in 2003 led to a wider range of disturbances and extreme conditions at the time.

Measurements further indicate that, depending on orbital characteristics, local time, and the underlying physical mechanisms of each occurrence, geomagnetic storms may have widely different impacts on low-Earth orbit (LEO) satellites. While the October storm reached a Kp of 8⁺, it was shorter in duration, and initial assessments based on products available via the ESA Space Weather Service Network suggest it may have been less impactful in terms of trapped radiation-induced effects on operations, compared to the May 2024 storm, which was characterized by Kp equal 9, sustained intensity and widespread impacts, including increased atmospheric drag [23] and radiation belts enhancement [10].

The 2024 space weather events present the most active periods of the Solar Cycle so far and the durability of modern satellite systems and operational practices to this level of event was clearly presented by the feedback received from all operators consulted in the preparation of this paper.

The importance of preserving long-term space weather records is emphasized by the analogy to the 2003 events. Taking into account also recent work done to characterise reasonable worst cases for space weather events, it is noted that more severe space weather conditions than those experienced in 2024 have been experienced by mission operators and should be expected in future. Conditions such as those experienced in both 2024 and 2003 may be used as the basis of training for operators and a wide range of data and tools exist to support this via the ESA SWE Service Portal and via other agencies internationally.

In order to increase readiness for upcoming extreme space weather events, the ESA Space Safety Programme is developing both enhanced space weather monitoring capabilities through missions such as Vigil and the Distributed Space Weather Sensor System (D3S) [44]. The Agency also develops and maintains the ESA Space Weather Service Network as a platform for Research-to-Operations-to-Research, enabling cross-disciplinary collaboration between operators working in affected sectors and domain experts to improve predictive capabilities and develop effective mitigation techniques for potentially damaging space weather activity. The network provides pre-operational services to a wide range of end users and actively encourages collaboration with spacecraft operators. This framework supports continuous exchange with operators where the real needs of the sector feed into future development planning and updates. This exchange supports continuous improvement and increases confidence that operations of critical infrastructure in space and on ground is resilient to future periods of extreme space weather.

Acknowledgements

The ESA SWE Service Network products presented in this paper form part of the European Space Agency's network of space weather services and service development activities, and are supported under ESA contract number 4000134036/21/D/MRP.

We therefore acknowledge all the institutions providing products and shown here: Solar Influences Data analysis Centre (SIDC) at the Royal Observatory of Belgium (ROB); British Geological Survey (BGS); IRF, The Swedish Institute of Space Physics; Universidad de Alcalá (UAH); Technical University of Denmark (DTU); Rutherford Appleton Laboratory (RAL Space); UK Met Office (UKMO); Collecte Localisation Satellites (CLS); ONERA; Space Applications & Research Consultancy (SPARC); the British Antarctic Survey and DH Consultancy in collaboration with the UK Met Office under contract from the European Space Agency; Athens Neutron Monitor Station of National and Kapodistrian University of Athens (NKUA); We acknowledge the NMDB database (www.nmdb.eu), founded under the European Union's FP7 programme (contract no. 213007) for providing data, and the relevant stations: ATHN, OULU, SOPO, SOPB, THUL; and the ESA Space Safety Programme.

For further information about space weather in the ESA Space Safety Programme see: www.esa.int/ . Access the ESA SWE portal here: <https://swe.ssa.esa.int>.

A special thank goes to Edmund Serpell and Peter Collins (ESA/OPS-OAG) for their support and their contribution with data and graphics on ESA Gaia mission and to Jutta Maria Huebner for providing the graphics for the Integral mission.

References

- [1] Lockwood, M., Owens, M. J., Brown, W., & Vázquez, M. (2024). The May 2024 Event in the Context of Auroral Activity over the past 375 years.
- [2] Elvidge, S., & Themens, D. (2024). The Probability of the May 2024 Solar Superstorm.
- [3] Diaz, J. (2024). Monitoring May 2024 solar and geomagnetic storm using broadband seismometers. *Scientific Reports*, 14(1), 1-13.
- [4] Grandin, M., Bruus, E., Ledvina, V. E., Partamies, N., Barthelemy, M., Martinis, C., ... & Bergstrand, C. (2024). The Gannon Storm: citizen science observations during the geomagnetic superstorm of 10 May 2024. *Geoscience Communication*, 7(4), 297-316.
- [5] Gonzalez-Esparza, J. A., Sanchez-Garcia, E., Sergeeva, M., Corona-Romero, P., Gonzalez-Mendez, L. X., Valdes-Galicia, J. F., et al. (2024). The mother's day geomagnetic storm on 10 May 2024: Aurora observations and low latitude space weather effects in Mexico. *Space Weather*, 22, e2024SW004111.
- [6] Kataoka, R., Nakano, S., & Uchino, S. (2024). Extended red aurora associated with super substorm igniting the October 10, 2024 magnetic storm as revealed by citizen science. *Authorea Preprints*.
- [7] Pesnell, W. D., & Schatten, K. H. (2018). An early prediction of the amplitude of solar cycle 25. *Solar Physics*, 293(7), 112.
- [8] Upton, L. A., & Hathaway, D. H. (2018). An updated solar cycle 25 prediction with AFT: The modern minimum. *Geophysical Research Letters*, 45(16), 8091-8095.
- [9] Foster, J. C., Erickson, P. J., Nishimura, Y., Zhang, S. R., Bush, D. C., Coster, A. J., ... & Franco-Diaz, E. (2024). Imaging the May 2024 extreme aurora with ionospheric total electron content. *Geophysical Research Letters*, 51(20), e2024GL111981.
- [10] Pierrard, V., Winant, A., Botek, E., & Péters de Bonhome, M. (2024). The Mother's Day Solar Storm of 11 May 2024 and Its Effect on Earth's Radiation Belts. *Universe*, 10(10), 391.
- [11] Kontogiannis, I. (2024). The extremely strong non-neutralized electric currents of the unique solar active region NOAA 13664. *Astronomy & Astrophysics*, 690, L10.

- [12] Jarolim, R., Veronig, A. M., Purkhart, S., Zhang, P., & Rempel, M. (2024). Magnetic Field Evolution of the Solar Active Region 13664. *The Astrophysical Journal Letters*, 976(1), L12.
- [13] World Data Center for Geomagnetism, Kyoto, M. Nose, T. Iyemori, M. Sugiura, T. Kamei (2015), Geomagnetic Dst index, doi:[10.17593/14515-74000](https://doi.org/10.17593/14515-74000)
- [14] Pulkkinen, A., Lindahl, S., Viljanen, A., & Pirjola, R. (2005). Geomagnetic storm of 29–31 October 2003: Geomagnetically induced currents and their relation to problems in the Swedish high-voltage power transmission system. *Space weather*, 3(8).
- [15] Kress, B. T., Mertens, C. J., & Wiltberger, M. (2010). Solar energetic particle cutoff variations during the 29–31 October 2003 geomagnetic storm. *Space Weather*, 8(5).
- [16] Panda, S. K., Gedam, S. S., Rajaram, G., Sripathi, S., Pant, T. K., & Das, R. M. (2014). A multi-technique study of the 29–31 October 2003 geomagnetic storm effect on low latitude ionosphere over Indian region with magnetometer, ionosonde, and GPS observations. *Astrophysics and Space Science*, 354, 267-274.
- [17] Nayak, C., Buchert, S., Yiğit, E., Ankita, M., Singh, S., Tulasi Ram, S., & Dimri, A. P. (2025). Topside Low-Latitude Ionospheric Response to the 10–11 May 2024 Super Geomagnetic Storm as Observed by Swarm: The Strongest Storm-Time Super-Fountain During the Swarm Era?. *Journal of Geophysical Research: Space Physics*, 130(3), e2024JA033340.
- [18] Tulasi Ram, S., Veenadhari, B., Dimri, A. P., Bulusu, J., Bagiya, M., Gurubaran, S., et al. (2024). Super-intense geomagnetic storm on 10–11 May 2024: Possible mechanisms and impacts. *Space Weather*, 22, e2024SW004126. <https://doi.org/10.1029/2024SW004126>
- [19] Mavromichalaki, H.; Papailiou, M.-C.; Livada, M.; Gerontidou, M.; Paschalis, P.; Stassinakis, A.; Abunina, M.; Shlyk, N.; Abunin, A.; Belov, A.; et al. Unusual Forbush Decreases and Geomagnetic Storms on 24 March, 2024 and 11 May, 2024. *Atmosphere* 2024, 15, 1033.
- [20] Ray, V., Berger, T. E., Waldron, Z. C., Sutton, E., Lucas, G., Knipp, D., ... & Scheeres, D. J. (2022). The impact of space weather on very low Earth orbit (VLEO) satellites. In *Advanced Maui Optical and Space Surveillance Technologies (AMOS) Conference* (p. 3).
- [21] www.esa.int/Enabling_Support/Operations/Double_trouble_Gaia_hit_by_micrometeoroid_and_solar_storm

- [22] Ashruf, A. M., Bhaskar, A., Vineeth, C., & Pant, T. K. (2024). Loss of 12 Starlink Satellites Due to Pre-conditioning of Intense Space Weather Activity Surrounding the Extreme Geomagnetic Storm of 10 May 2024. *arXiv preprint arXiv:2410.16254*.
- [23] Parker, W. E., & Linares, R. (2024). Satellite drag analysis during the may 2024 Gannon geomagnetic storm. *Journal of Spacecraft and Rockets*, 61(5), 1412-1416.
- [24] Belian, R. D., Cayton, T. E., & Reeves, G. D. (1995). Quasi-periodic global substorm generated flux variations observed at geosynchronous orbit. *Geophysical Monograph Series*, 86, 143.
- [25] Cai, X., & Clauer, C. R. (2009). Investigation of the period of sawtooth events. *Journal of Geophysical Research: Space Physics*, 114(A6).
- [26] Cai, X., Zhang, J. C., Clauer, C. R., & Liemohn, M. W. (2011). Relationship between sawtooth events and magnetic storms. *Journal of Geophysical Research: Space Physics*, 116(A7).
- [27] Das, S. K., Stolle, C., Yamazaki, Y., Rodríguez-Zuluaga, J., Wan, X., Kervalishvili, G., ... & Perwitasari, S. (2024). On the F-region ionospheric plasma density distribution and irregularities response during the May-2024 geomagnetic storm observed by LEO satellites. *Authorea Preprints*.
- [28] Oliveira, D. M., Zesta, E., & Nandy, D. (2025). The 10 October 2024 geomagnetic storm may have caused the premature reentry of a Starlink satellite. *Frontiers in Astronomy and Space Sciences*, 11, 1522139.
- [29] Siemes, C., Borries, C., Bruinsma, S., Fernandez-Gomez, I., Hładczuk, N., den IJssel, J., ... & Visser, P. (2023). New thermosphere neutral mass density and crosswind datasets from CHAMP, GRACE, and GRACE-FO. *Journal of Space Weather and Space Climate*, 13, 16.
- [30] Kornfeld, R. P., Arnold, B. W., Gross, M. A., Dahya, N. T., Klipstein, W. M., Gath, P. F., & Bettadpur, S. (2019). GRACE-FO: the gravity recovery and climate experiment follow-on mission. *Journal of spacecraft and rockets*, 56(3), 931-951.
- [31] Evans, J. S., Correira, J., Lumpe, J. D., Eastes, R. W., Gan, Q., Laskar, F. I., ... & Veibell, V. (2024). GOLD observations of the thermospheric response to the 10–12 May 2024 Gannon superstorm. *Geophysical Research Letters*, 51(16), e2024GL110506.

- [32] Ranjan, A. K., & Pallamraju, D. (2025). Latitudinal distribution of thermospheric nitric oxide (NO) infrared radiative cooling during May and October 2024 geomagnetic storms. *Journal of Geophysical Research: Space Physics*, 130(3), e2024JA033559.
- [33] Panasyuk, C. S. E. E. I. 2. M., Kuznetsov, S. N., Lazutin, L. L., Avdyushin, S. I., Alexeev, I. I., Ammosov, P. P., ... & Yushkov, B. Y. (2004). Magnetic storms in October 2003. *Cosmic research*, 42, 489-535.
- [34] De Franceschi, G., Alfonsi, L., Romano, V., Aquino, M., Dodson, A., Mitchell, C. N., ... & Wernik, A. W. (2008). Dynamics of high-latitude patches and associated small-scale irregularities during the October and November 2003 storms. *Journal of Atmospheric and Solar-Terrestrial Physics*, 70(6), 879-888.
- [35] Cid, C., Palacios, J., Saiz, E., Guerrero, A., & Cerrato, Y. (2014). On extreme geomagnetic storms. *Journal of Space Weather and Space Climate*, 4, A28.
- [36] Plunkett, S. P. (2005). The extreme solar storms of October to November 2003. *Naval Res. Lab. Rev.*, 91-98.
- [37] Gopalswamy, N., Yashiro, S., Liu, Y., Michalek, G., Vourlidas, A., Kaiser, M. L., & Howard, R. A. (2005). Coronal mass ejections and other extreme characteristics of the 2003 October–November solar eruptions. *Journal of Geophysical Research: Space Physics*, 110(A9).
- [38] Ranjan, A. K., Nailwal, D., Sunil Krishna, M. V., Kumar, A., & Sarkhel, S. (2024). Evidence of potential thermospheric overcooling during the May 2024 geomagnetic superstorm. *Journal of Geophysical Research: Space Physics*, 129, e2024JA033148.
- [39] United States, National Weather Service, (2004). Intense space weather storms October 19–November 07, 2003.
- [40] Berger, T. E., Holzinger, M. J., Sutton, E. K., & Thayer, J. P. (2020). Flying through uncertainty. *Space Weather*, 18(1), e2019SW002373.
- [41] Barbieri, L. P., & Mahmot, R. E. (2004). October–November 2003's space weather and operations lessons learned. *Space Weather*, 2(9).
- [42] Hapgood, M. (2018). Linking space weather science to impacts—the view from the Earth. In *Extreme events in Geospace* (pp. 3-34). Elsevier.

[43] Fry, E. K. (2012). The risks and impacts of space weather: Policy recommendations and initiatives. *Space Policy*, 28(3), 180-184.

[44] Heil, M., Luntama, J. P., Kraft, S., & Glover, A. (2023). *ESA's space weather monitoring system* (SpaceOps-2023, ID #652). Paper presented at the 17th International Conference on Space Operations, Dubai, United Arab Emirates, 6–10 March 2023. European Space Agency.